Journal of Neuroimmunology 328 (2019) 5–19

Contents lists available at ScienceDirect

Journal of Neuroimmunology

journal homepage: www.elsevier.com/locate/jneuroim

Syngeneic, in contrast to allogeneic, mesenchymal stem cells have superior therapeutic potential following spinal cord injury

Ramil Hakim[b,c], Ruxandra Covacu[b,c], Vasilios Zachariadis[d], Arvid Frostell[c], Sreenivasa Sankavaram[b,c], Mikael Svensson[a,c,*,1], Lou Brundin[a,b,c,1]

[a] Department of Neurology and Neurosurgery, Karolinska University Hospital, BioClinicum, Solnavägen 30, Solna, Stockholm 17176, Sweden
[b] Center for Molecular Medicine, Karolinska Institutet, Solna 17176, Stockholm, Sweden
[c] Department of Clinical Neuroscience, Karolinska Institutet, Solna 17176, Stockholm, Sweden
[d] Department of Oncology and Pathology, Karolinska Institutet, Solna 17176, Stockholm, Sweden

ARTICLE INFO

Keywords:
Spinal cord injury
Mesenchymal stem cell
Histocompatibility
Neuroinflammation
Hind limb function
Graft survival
Immune response

ABSTRACT

We evaluated the importance of histocompatibility of transplanted MSCs in terms of therapeutic potential. Mouse syngeneic MSCs or allogeneic MSCs were transplanted following SCI in mouse. In this study we found that syngeneic, but not allogeneic, MSCs alternatively activated macrophages resulting in a down-regulation of pro-inflammation. Syngeneic MSCs also had a general suppressive effect on the immune response as compared to allogeneic MSCs. Additionally, syngeneic, but not allogeneic, MSCs significantly enhanced the recovery of hind limb function. In this study we show that the histocompatibility of transplanted MSCs is of importance for their therapeutic potential.

1. Introduction

A traumatic spinal cord injury (SCI) is a consequence of external forces with a detrimental impact on the spinal cord (Ahuja et al., 2017). Although intense research efforts have been made, for the time being, no curative treatment for this devastating condition exists.

Mesenchymal stem cells (MSCs) are plastic adherent, fibroblast-like cells with the ability to self-renew and differentiate along the mesodermal-lineage (Araña et al., 2013). MSCs express CD105, CD44, CD90 (Aras et al., 2016; Berglund and Schnabel, 2017; Cantinieaux et al., 2013), CD29 and Sca1 and lack expression of CD11b, CD34 and CD45 (Berglund and Schnabel, 2017; Cantinieaux et al., 2013). MSCs transplanted following experimental SCI alternatively activate macrophages (Canton et al., 2013; Chan et al., 2008) down-regulate pro-inflammation (Chen et al., 2015; Cízková et al., 2006; Friedenstein et al., 1974) and enhance recovery of hind limb locomotor function (Chen et al., 2015; Gu et al., 2010; Han et al., 2015; Himes et al., 2006; Isakova et al., 2014; Iwamoto et al., 1994; Jung et al., 2009; Kim et al., 2015; Klyushnenkova et al., 2005; Le Blanc et al., 2003; Liu et al., 2012; Martini et al., 2010; Melief et al., 2013). However, MSCs express MHC-I on the cell surface and MHC-II within the cell (Cantinieaux et al., 2013). MSCs have therefore been considered immune-privileged (Berglund and Schnabel, 2017; Cantinieaux et al., 2013; Melo et al., 2017; Menezes et al., 2014; Morita et al., 2016). The expression of these molecules is up-regulated following exposure to IFNγ and IL1β in vitro (Cantinieaux et al., 2013; Melo et al., 2017; Morita et al., 2016; Naglich et al., 1992; Nakajima et al., 2012; Okuda et al., 2017). MHC-mismatched transplantation has been reported to result in expansion of NK, B -and T cells. MHC-mismatched cells may also induce B cells to release cytotoxic antibodies with lethal effects on grafted MSCs (Morita et al., 2016; Osaka et al., 2010; Park et al., 2012). The degree of immune response seem to be determined by the degree of MHC-I -and II mismatch (Park et al., 2012). Furthermore, allogeneic but not syngeneic MSCs, have been reported to be rejected following transplantation (Prigozhina et al., 2008; Quertainmont et al., 2012).

The immune response that follows a SCI is most substantial during the acute and subacute phase. Considering the immunomodulatory capacity of MSCs, transplantation as early as possible is likely to be most beneficial. However, establishment and verification of autologous MSCs exceed this phase in terms of time. Allogeneic transplantation remains the only feasible option during this time period. Although MSCs have been characterized in detail in vitro, the importance of

* Corresponding author at: Karolinska University Hospital, BioClinicum, Solnavägen 30, 171 64, Solna, Stockholm, Sweden.
E-mail addresses: ramil.hakim@ki.se (R. Hakim), ruxandra.covacu@ki.se (R. Covacu), vasilios.zachariadis@ki.se (V. Zachariadis), arvid.frostell@ki.se (A. Frostell), sreenivasa.sankavaram@ki.se (S. Sankavaram), mikael.svensson@ki.se (M. Svensson), lou.brundin@ki.se (L. Brundin).
[1] These authors contributed equally.

https://doi.org/10.1016/j.jneuroim.2018.11.005
Received 11 October 2018; Received in revised form 6 November 2018; Accepted 7 November 2018

histocompatibility of transplanted MSCs in terms of therapeutic potential has not been investigated in much detail. By screening the transcriptome of spinal cords in animals grafted with MSCs with different haplotypes the importance of histocompatibility in terms of therapeutic potential might be better understood.

Therefore, in this project we aimed to comprehensively evaluate the role of histocompatibility of transplanted MSCs on their therapeutic potential. We hypothesized that syngeneic MSCs may have superior therapeutic potential as compared to allogeneic MSCs following experimental SCI. We found that syngeneic MSCs activated macrophages alternatively while allogeneic MSCs activated macrophages classically which resulted in syngeneic MSCs down-regulating pro-inflammation while allogeneic MSCs did the opposite. Syngeneic MSCs also down-regulated the general immune response measured using global transcriptional analysis, enhanced recovery of hind limb motor function and had superior survival.

2. Materials and methods

2.1. Mice

Wild-type inbreed mice (C57BL/6 J and BALB/c, 6–8 w, 16–20 g) were purchased from Scanbur (Stockholm, Sweden). Mice were kept in a humidified room with a 12:12 h light-dark cycle at 21 °C with constant access to food and water. Animal experiments were approved by the local ethical committee (Stockholm, Sweden) and conducted according to ethical permits: N38/16, N196/15 and N124/15.

2.2. Experimental contusion spinal cord injury

Animals were acclimatized to the surgical room 3–5 days prior to surgical intervention. C57BL/6J mice were used as hosts for injury and cell transplantation in all experimental groups. Anesthesia was induced by administration of 0.5 mg/kg medetomidin i.p. (Domitor ® vet., Orion Pharma Animal Health, 1 mg/ml) and 75 mg/kg ketamine i.p. (Ketador vet., Salfarm Scandinavia, 100 mg/ml) in combination with analgesics: 0.05 mg/kg buprenorfin s.c. (Temgesic®, Indivior 0.3 mg/ml) and 5 mg/kg karprofen s.c. (Rimadyl® vet. Orion Pharma Animal Health, 50 mg/ml). Prior to surgery the mice were weighed, eyes were covered with cerate (Oculentum simplex APL, Apotek Produktion & Laboratorier), 0.1 ml normal saline was given s.c. and the fur on the back was gently removed. The skin was incised, the muscle layers were carefully separated and the vertebral column mounted using bilateral fixators in a stereotaxic frame (Model 900 & 900-c, Kopf ®). The mouse was kept on a heating pad during the entire procedure. Laminectomy was conducted using a high speed 2 mm diamond drill (Anspach ®, EMAX® 2) and the dura mater was opened using a micro dissector. A 75 kdyn contusion spinal cord injury (SCI) was induced at thoracic level 10 using a computer controlled impactor (Infinite Horizon, IH-0400). The wound was closed using running and simple sutures (Vicryl, 4.0). Analgesics, as described above, were once again administrated post-operatively. Buprenorfin was administrated morning and evening, while karprofen was given once daily for the 3 first days following surgery. The urine bladder was manually compressed twice daily until recovery of reflexive bladder function appeared. Animals were weighed once weekly and a weight loss of 25% or more was used as the humane endpoint.

2.3. Mouse bone marrow mesenchymal stem cells

Bone marrow mesenchymal stem cells (MSCs) were established from C57BL/6J and BALB/c mice. BALB/c mice were used as MSC donors only. Animals were euthanized by administration of a lethal dose of pentobarbital i.p. (Pentobarbitalnatrium vet. APL, 60 mg/ml) followed by decapitation. The carcass was rinsed in 70% ethanol and the hind limbs were removed and stored in HBSS (Gibco™, 14170112) with 1:50 Penicillin-Streptomycin (Pen-Strep) (Gibco ®, 10.000 U/ml, 15140122) on ice. Tibia and femur were dissected bilaterally and stored in HBSS with 1:50 Pen-Strep on ice. The epiphysis of the collected tibias and femurs were cut at each end. The bone marrow was then extruded by flushing with pre-warmed basal medium (89% α-MEM (Gibco ®, 22561054), 1% Pen-Strep, 10% fetal bovine serum, FBS, (Gibco ®, 10082147)) using a 27 gauge needle. The collected bone marrow was dissociated by passaging multiple times through a 18 gauge needle and finally filtered through a 70 μm cell strainer (Corning, Inc., 352350). Bone marrow cells were re-suspended in basal medium and plated at a density of 1.45×10^6 cells/cm^2 in 100 mm tissue culture treated cell culture dishes (150350, Nunc™) and cultured in a humidified chamber at 37 °C and 5% CO_2. 8–10 days post initial plating the plastic adherent bone marrow cells were harvested for depletion of CD34 +, CD45 + and CD11b + cells (Suppl. Methods). MSCs were carefully evaluated and characterized prior to transplantation (Suppl. Methods, Suppl. Fig. 1A-F, Suppl. Results).

2.4. Expression construct and transfection of mesenchymal stem cells

MSCs were transfected using a non-integrating, self-replicating enhanced episomal vector system (Cat# EEV600A-1, System Biosciences) containing a cDNA sequence of the *HBEGF/DTR* (Ritfeld et al., 2012), (Ryu et al., 2012) linked to the mCherry gene via a sequence for a 2a self-cleaving peptide linker (synthesized at Eurofins Genomics). The sequence was cloned, using standard molecular cloning techniques, into the multiple cloning site (MCS) located downstream of the CAGs promoter in the EEV (Suppl. Fig. 2A). The DTR was not utilized in this study. Endotoxins were removed from the plasmid using the EndoFree Plasmid Maxi Kit (Qiagen, 12362) using manufacturer's instructions. MSCs were plated at 10.000 cells/cm^2 in 6-wells. Following 48 h of incubation the MSCs were transfected using Lipofectamine™ 3000 (Invitrogen, L3000001) using manufacturer's protocol. 2.5 μg cDNA was used for each 6-well. After 48 h of additional incubation the fluorescence was confirmed using a microscope (Zeiss, Axiovert 200) (Suppl. Fig. 2B), the cells were washed in 1xDPBS, harvested, re-suspended in 4 μl α-MEM and stored in 0.2 ml Eppendorf tubes at 4 °C until transplantation. Transfected, non-harvested, MSCs expressed mCherry for at least 3 weeks in culture.

2.5. Mouse stromal vascular fraction

Subcutaneous adipose tissue from mice was dissected and kept in 1:50 Pen-Strep in HBSS on ice. The adipose tissue was minced using two scalpels (Kiato, 23124) and dissociated by incubation for 1 h in 2 mg/ml Collagenase P (Sigma, 11213857001) at 37 °C. After homogenization the suspension was passed through a 100 μm cell strainer (Corning, Inc., 352360) followed by a 40 μm cell strainer (Corning, Inc., 352340). Cells were collected by centrifugation at 600 ×*g* for 7 min and re-suspended in 1 ml basal medium. Cells were incubated in 3 ml ACK lysis buffer (Gibco®, A1049201) for 5 min at RT. Cells were washed in 10 ml 1× DPBS and collected by centrifugation at 600 ×*g* for 5 min, counted and re-suspended in α-MEM prior to transplantation (Schnabel et al., 2014). mSVFs were transplanted in one of the experimental groups and served as control to the transplanted MSCs.

2.6. Transplantation

24 h post SCI the mice were re-anesthetized and the sutures re-opened. A total of 0.5×10^6 MSCs, diluted in 5 μl α-MEM, were transplanted using a glass capillary needle (WPI, 1B150F-6) prepared using a pipette puller (HEKA, PIP5) attached to a 10 μl syringe (Hamilton ®, 80330) into the epicenter of the injury. The glass capillary needle and syringe were attached to a stereotaxic frame and the injections were made under a surgical microscope to ensure accuracy. The skin was re-sutured (Vicryl, 4.0) and post-operative procedures were implemented.

2.7. Assessment of recovery of hind limb function

Recovery of stepping ability and muscular tonus was assessed at 3, 7, 14, 21, 28, 35, 42, 49 and 70 days post SCI using the iliac crest and trochanter major height index. The iliac crest was unmasked by removing the fur using a hair trimmer prior to labelling the iliac crest and trochanter major using fluorescent dye. The mice were recorded in a custom built plexiglass runway with reinforcing illumination (Euromex, LE.5210) using a remote controlled Canon EOS 6D. Two to four passes per hind limb was recorded for each mouse. Video recordings were analyzed off-line using ClickJoint 5.0 (ALEA Solutions GmbH) (Schu et al., 2012).

2.8. Harvesting and collection of spinal cord and cerebrospinal fluid

3, 10, 20 and 70 days post SCI the mice were given a lethal dose of pentobarbital. Time points for sacrifice were empirically determined (Suppl. Fig. 3A-B, Suppl. Results). Using a glass capillary needle attached to a 10 µl Hamilton ® syringe, the cerebrospinal fluid (CSF) was aspirated from the cisterna magna, placed in an Eppendorf tube and snap-frozen in liquid nitrogen. The spinal cord injury epicenter (+/− 3 mm in cranial/caudal direction) was dissected and collected under a surgical microscope. Spinal cords in which gene expression was to be evaluated were placed in an Eppendorf tube, snap-frozen in liquid nitrogen and stored at −80 °C until down-stream processing. Animals used for fluorescence activated cell sorting were perfused with NaCl using a peristaltic pump (Watson Marlow, 120S) and the spinal cords were stored in 1xPBS on ice until down-stream processing. Mice intended for immunohistochemistry were perfused with 4% paraformaldehyde following perfusion with NaCl and spinal cords were post-fixed in 4% PFA at 4 °C over-night.

2.9. Fluorescence activated cell sorting

Dissected spinal cords were dissociated using trituration in pre-heated 10 U/ml papain (Worthington, L5003126) at 37 °C. DNAse 200 U/ml (Sigma, D7291) was added at the end of the dissociation. Papain was inactivated using 1% BSA (Gibco®, 15260–037). Myelin was removed by adding 30% Percoll (Sigma, P1644) in 1xDPBS and centrifugation at 750 ×*g* for 10 min at 4 °C with slow brake. The pellet was re-suspended in FACS-buffer (1% BSA, 2 mM EDTA (Gibco ®, 15575–038), 25 mM HEPES (Sigma, H0887) and filtered through a pre-wet 100 µm cell strainer, followed by a 40 µm cell strainer, and washed in FACS-buffer one final time. 1 µg Mouse Fc Block (CD16/CD32) (BD, 553141) per 1×10^6 cells in 100 µl FACS-buffer was added followed by incubation on ice for 5 min. 5 µl of pre-conjugated antibody (Table 1) was added to 1×10^6 cells in 100 µl FACS-buffer and incubated for 20 min at RT. Following wash and centrifugation, the cells were re-suspended in 0.5 ml FACS-buffer. FACS was conducted using BD Influx™ cell sorter. Sorted cells were collected by centrifugation at 300 ×*g* for 5 min and re-suspended in 0.5 ml Trizol reagent (Thermo Fisher, 15596026) and stored at −80 °C until down-stream processing.

2.10. RNA isolation and cleanup

2.10.1. Spinal cords and differentiated mesenchymal stem cells

Total RNA from spinal cords was isolated using RNeasy mini kit (Qiagen, 74104) while RNA from differentiated MSCs was isolated using the RNeasy micro kit (Qiagen, 74004). 1% β-mercaptoethanol was added to the lysing buffer prior to mechanical grinding (IKA ® T8.01). Contaminating genomic DNA was removed during the isolation by on-column digestion with DNase (DNase I Qiagen, 79254). RNA was diluted in nuclease-free H_2O and stored at −80 °C until down-stream analysis.

2.10.2. Isolated microglia/macrophages and monocyte populations

RNA isolation was performed according to manufacturer's (Trizol reagent) instructions. The isopropanol precipitation step together with 20 µg glycogen was performed over-night. RNA clean-up was performed using RNeasy micro kit (Qiagen, 74004) according to manufacturer's protocol. RNA was diluted in nuclease-free H_2O and stored in −80 °C until downstream analysis.

2.11. Reverse transcription and real-time quantitative polymerase chain reaction

2.11.1. Spinal cords and differentiated mesenchymal stem cells

500 ng RNA was reverse-transcribed in a 20 µl reaction using iScript™ cDNA Synthesis Kit (Bio-Rad, 1708891) using a block heater (Eppendorf™ ThermoStat Plus, 022670204) according to manufacturer's instructions and finally diluted 1:5 in RNase-free water (Sigma, W4502). Purified cDNA was used as template in a 10 µl RTqPCR reaction with iQ™ SYBR® Green Supermix (Bio-Rad, 170–8887) and 5 µM forward and reverse primers (Table 2). RTqPCR was performed with a CFX384 Touch™ Real-Time PCR detection System (Bio-Rad, 1855485) at 95 °C for 3 min; 40 cycles at 95 °C for 10 s; at 60 °C for 30 s and 72 °C for 30 s. Each reaction was performed in duplicate. The ΔΔCt method was used for analysis. Expression was normalized to the expression of GAPDH and Actin-β in Bio-Rad CFX manager (version 3.1, Bio-Rad Laboratories Inc.).

2.11.2. Isolated microglia/macrophages and monocyte populations

RNA was reverse-transcribed using the protocol used for spinal cords. Prior to RTqPCR the cDNA was pre-amplified using TaqMan Assay (20x) (Table 2) and SsoAdvanced™ PreAmp Supermix (Bio-Rad, 172–5160) using manufacturer's protocol at 95 °C for 3 min; 15 cycles at 95 °C for 15 s; 58 °C for 4 min. Samples were diluted 1:5 in TE buffer (Qiagen). RTqPCR was then performed in a 10 µl reaction with SsoAdvanced™ Universal Probes Supermix (Bio-Rad, 172–5280), 1 µl TaqMan assay (20x), 2 µl template and 2 µl nuclease-free H_2O at 95 °C for 30 s; 40 cycles at 95 °C for 10 s; 60 °C for 20 s. The ΔΔCt was used for analysis and the expression was normalized to the expression of Actin-β in Bio-Rad CFX manager (version 3.1, Bio-Rad Laboratories Inc.).

Table 1
Primary, secondary and pre-conjugated antibodies.

Antibody type	Target	Product	Dilution
Primary	α-Iba1	Abcam (ab5076)	1:400
	α-NeuN	Merck (MAB377)	1:1000
Counterstain	Hoechest 33258	Invitrogen (H1398)	1:10000 (10 mg/ml stock)
Secondary	α-goat (Alexa 488)	Life technologies (A11055)	1:200
	α-mouse (Alexa 488)	Life technologies (A11001)	1:1000
Pre-conjugated	α-CD45 (PE/Cy7)	BD (552848)	1 mg/1e6 cells (0.2 mg/ml stock)
	α-CD11b (PE)	Biolegend (101208)	
	α-CD64 (PerCP/Cy5.5)	Biolegend (139308)	
	α-Ly6G (v450)	BD (560603)	

Table 2
Primers and probes for RTqPCR.

A. Primers

Usage	Target	Manu-facturer	Sense	Antisense
Validation of mesodermal differentiation of MSCs	Adipsin	Eurofins Genomics	ATGGTATGATGTGCAGAGTGTAG	CACACATCATGTTAATGGTGAC
	Lipoprotein lipase		GAGGACACTTGTCATCTCATTC	CCTTCTTATTGGTCAGACTTCC
	Bone sialoprotein		CAAGCGTCACTGAAGCAGGTG	CATGCCCCTTGTAGTAGCTGTATT
	Cathepsin K		TGCCTTCCAATACGTGCAGCA	TGCATTTAGCTGCCTTTGCCG
	CBFA1		CCGCACGACAACCGCACCAT	CGCTCCGGCCCACAAATCTC
	Osteonectin		AGCGCCTGGAGGCTGGAGAC	CTTGATGCCAAAGCAGCCGG
	Osteopontin		CAGTGATTTGCTTTTGCCTGTTTG	GGTCTCATCAGACTCATCCGAATG
	Sox9		CTCTGGAGGCTGCTGAACG	TTGTAATCGGGGTGGTCTTTCTT
	Actin-β		TGGAATCCTGTGGCATCCATGAAAC	TAAAACGCAGCTCAGTAACAGTCCG
	GAPDH		AAGGGCTCATGACCACAGTC	CAGGGATGATGTTCTGGGCA
Neuro-inflammation in spinal cord	CCL2		GCTCAGCCAGATGCAGTTA	TACGGGTCAACTTCACATTC
	CCL3		CCATGACACTCTGCAACCAA	CGTGGAATCTTCCGGCTGTA
	CCL4		TGCTCGTGGCTGCCTTCT	CAGGAAGTGGGAGGGTCAGA
	CCL5		GACAGCACATGCATCTCCCA	CCTTCGAGTGACAAACACGACT
	CCL11		GGCTGACCTCAAACTCACAGAAA	ACATTCTGGCTTGGCATGGT
	CXCL1		CTGGGATTCACCTCAAGAACATC	CAGGGTCAAGGCAAGCCTC
	GM-CSF		CTGTCACGTTGAATGAAGAGGT	GGCTTCCTCATTTTTGGCCT
	IFNγ		AGCTGATCCTTTGGACCCTC	GTCACCATCCTTTTGCCAGTT
	IL1β		CTGTGTCTTTCCCGTGGACC	CAGCTCATATGGGTCCGACA
	IL3		TGCGCTGCCAGGGGTCTT	ATTCCACGGTTCCACGGTTAGG
	IL5		GACAAGCAATGAGACGATGA	GAACTCTTGCAGGTAATCCA
	IL6		TAGTCCTTCCTACCCCAATTTCC	TTGGTCCTTAGCCACTCCTTC
	IL10		ACCTGGTAGAAGTGATGCCC	ACAGGGGAGAAATCGATGACA
	IL12a		CCAAACCAGCACATTGAAGA	AGCTCCCTCTTGTTGTGGAA
	IL12b		GGGACATCATCAAACCAGACCC	GCCTTTGCATTGGACTTCGG
	TNFα		AAGCCTGTAGCCCACGTCGTA	GGCACCACTAGTTGGTTGTCTTTG
	Actin-β		TGGAATCCTGTGGCATCCATGAAAC	TAAAACGCAGCTCAGTAACAGTCCG
	GAPDH		AAGGGCTCATGACCACAGTC	CAGGGATGATGTTCTGGGCA
M1/M2 ratio in spinal cord	CD16		TTTGGACACCCAGATGTTTCAG	GTCTTCCTTGAGCACCTGGATC
	CD32		AATCCTGCCGTTCCTACTGATC	GTGTCACCGTGTCTTCCTTGAG
	CD206		TCTTTGCCTTTCCCAGTCTCC	TGACACCCAGCGGAATTTC
	Arg1		TTGGGTGGATGCTCACACTG	TTGCCCATGCAGATTCCC

B. Probes

Usage	Target	Manufacturer	Amplicon size (bp)	Assay ID
M1/M2 ratio in macrophages/monocytes isolated from spinal cord	Actin-β	Thermo Fisher	143	Mm02619580_g1
	Fcgr3 (CD16)		90	Mm00438882_m1
	Mrc1 (CD206)		147	Mm01329361_m1
	Arg1		65	Mm00475988_m1
	Fcgr2b (CD32)		77	Mm00438875_m1

2.12. RNA-sequencing

Sequencing libraries were prepared from total RNA, digested of DNase, using TruSeq stranded mRNA library preparation kit with polyA selection (Illumina Inc.). Libraries were sequenced 125 cycles paired-end in one lane using the HiSeq2500 system and v4 sequencing chemistry (Illumina Inc.) to a combined total of at least 180×10^6 read-pairs (15 M/sample) with at least 75% of the bases having a base quality score of 30 or higher. Low quality regions and adapter sequences were removed using TrimGalore (Babraham Bioinformatics). Remaining pair-end reads were aligned to the mouse genome (build GRCm38) using the splice-aware aligner STAR. Read counts were summarized over genes using featureCounts and Ensembl annotation release 81. Differential gene expression analysis was conducted in *R* (version 3.3.2) using 'limma' and 'edgeR' with annotations from 'Mus.musculus', available through https://www.bioconductor.org/. Functional analysis was conducted using overrepresentation enrichment analysis using gene ontology and Kyoto Encyclopedia of Genes and Genomes terms.

2.13. Immunoassay

Cytokine and chemokine expression in the cerebrospinal fluid was analyzed using Bio-Plex Pro™ Mouse Cytokine 23-plex Assay (Bio-Rad Laboratories, Hercules, CA, USA) and a Bio-Plex ® MAGPIX (Bio-Rad Laboratories, Hercules, CA, USA) using manufacturer's protocol.

2.14. Immunohistochemistry

Following post-fixation the spinal cords were cryo-protected in 15% and 30% sucrose (Sigma, S9378) in 1xPBS. Spinal cords were placed in 25 × 20 × 5 mm cryomolds (Tissue-Tek® Cryomold®, 420572) using compound (Tissue-Tek® O.C.T.™) and frozen to −60 °C. 20 µm coronal sections were produced using a cryostat (Leica, CM1850) and mounted on adhesion slides (VWR, SuperFrost® Plus, 48311–703). Sections were thawed and rehydrated ~20 min in 1xPBS at RT. Sections were blocked for 2 h in RT in blocking solution (0.3% Triton X-100 (Sigma, 93443), 5% normal donkey serum (Millipore, S30–100), 1xPBS and sodium azide (Sigma, S-2002). In the blocking solution for NeuN, normal donkey serum was replaced by normal goat serum (Serotec, 301104) and 3% BSA (Sigma, A4503). Following rinse, sections were incubated in primary antibody (Table 1) at 4 °C for 24 h. Sections were rinsed in 1xPBS and incubated in secondary antibody (Table 1) at RT for 1 h. Finally, nucleic acid stain (Table 1) was added and sections were incubated at RT for 10 min.

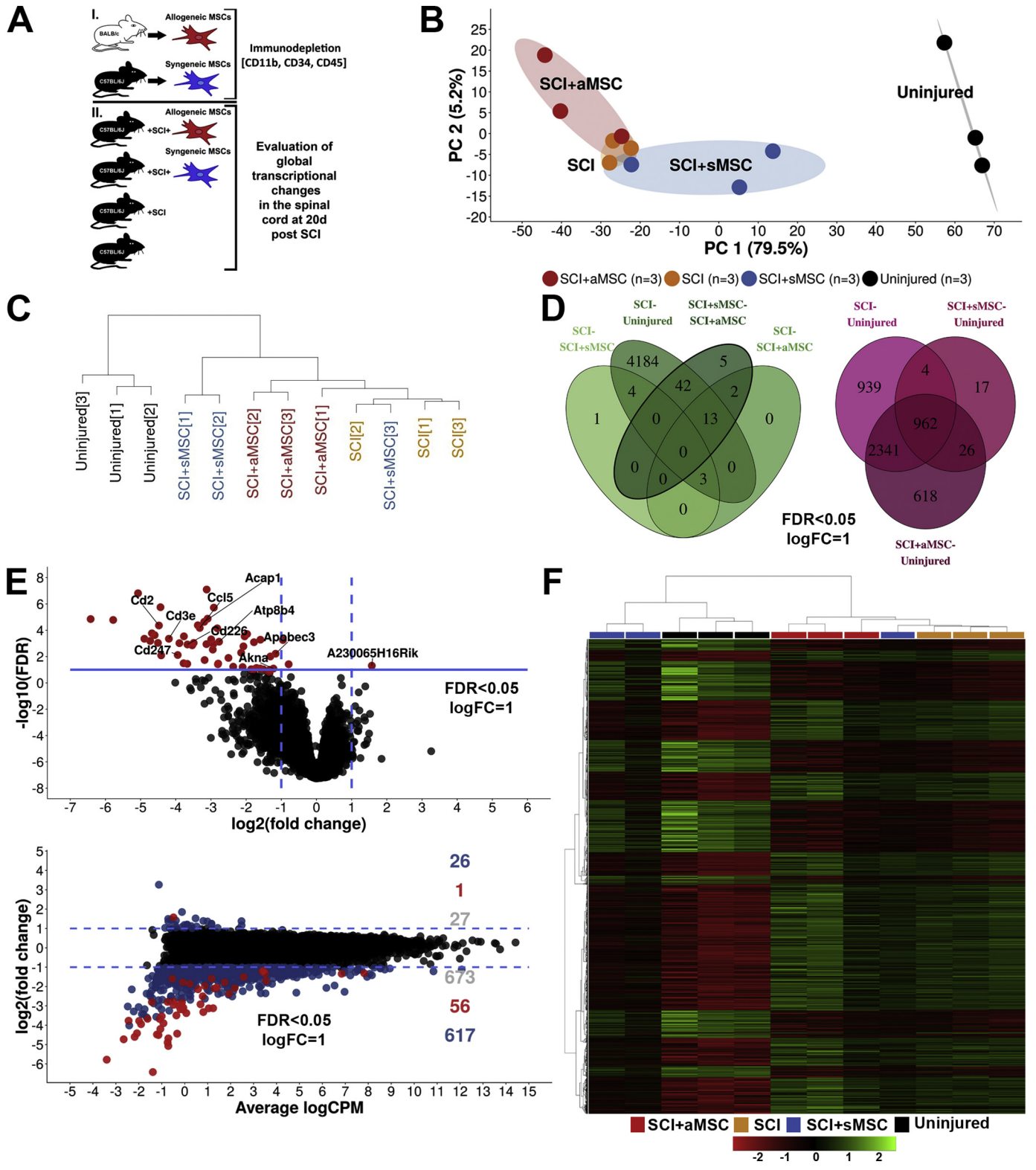

Fig. 1. Global transcriptional changes in the spinal cord - differential gene expression.
Fig. 1A experimental design. I) Establishment of allogeneic mesenchymal stem cells (aMSC) and syngeneic MSCs (sMSC), II) experimental groups. Fig. 1B multi-dimensional scaling plot of the first and second principal component following a principal component analysis using the 500 genes with highest inter-sample variance. Each dot represents a biological replicate. Ellipse represents a 95% confidence interval around replicates. Fig. 1C agglomerative hierarchical clustering of biological replicates using the 1000 genes with the highest inter-sample variance. Fig. 1D differentially expressed genes in each contrast. Fig. 1E volcano (top) and mean-difference (bottom) plot for contrast: SCI + sMSCs vs SCI + aMSCs. Blue dots represent genes fulfilling: [(logFC > 1 OR logFC < −1)] while red dots represent genes fulfilling: [(logFC > 1 OR logFC < −1) AND FDR < 0.05]. Fig. 1F heat map representation of significantly differentially expressed genes in all contrasts using row –and column wise hierarchical clustering.

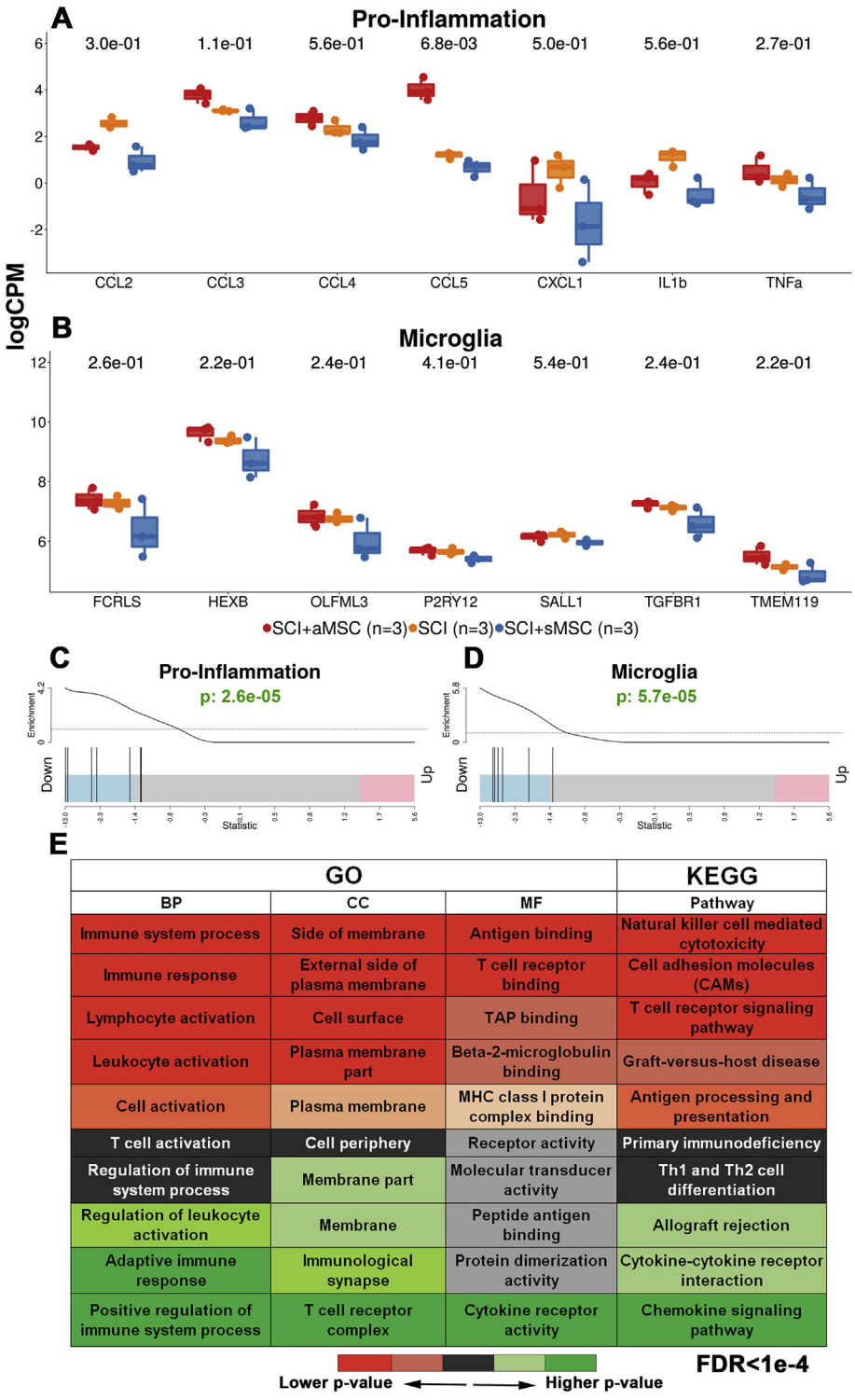

Fig. 2. Global transcriptional changes in the spinal cord – functional analysis.
Fig. 2A, B logCPM values for genes defining pro-inflammation and microglia. Numeric values in plot represent FDR following comparison between all three experimental groups for each gene separately. Each dot represents one biological replicate. Fig. 2C, D barcode plots entailing the enrichment of gene sets in Fig. 2A, B for contrast: SCI + sMSC vs SCI + aMSC. *P*-value following competitive gene set testing accounting for inter-gene correlation reported for the same contrast and set of genes. Fig. 2E significant gene ontology (GO) and Kyoto Encyclopedia of Genes and Genomes (KEGG) terms for contrast: SCI + sMSCs vs SCI + aMSCs (based on genes fulfilling FDR < 0.05, logFC = 1). The terms are ranked and color labelled based on their *p*-values. *BP = biological process, CC = cellular component, MF = molecular function.*

2.15. Confocal microscopy

Stained sections of the spinal cord were imaged using a confocal microscope (Zeiss LSM 880 Airyscan). Five random 20× images were taken from each quadrant surrounding the epicenter of the injury for every other section when quantifying NeuN+ and Iba1+ cells. All mCherry+MSCs were captured when evaluating MSC survival.

2.16. Automatic cell quantification

Automatic cell quantification was conducted in Image Processing and Analysis in Java (ImageJ, 64-bit Java 1.6.0_24). For each animal and staining/fluorescence (Iba1, NeuN, mCherry) the images were imported and converted to an image sequence. The cell count was estimated using a custom built macro. Briefly, the macro splits each image in the image sequence into its 3 color channels. The selected channels (of interest) are then multiplied. The product image is converted to a binary image which is then subjected to water shedding.

Table 3
Overrepresentation enrichment analysis.

GO				KEGG		
Term	Ont	Genes	P-Value (Down)	Pathway	Genes	P-Value (Down)
Immune system process	BP	37	1.03e−22	Natural killer cell mediated cytotoxicity	11	2.65e−12
Immune response	BP	29	7.79e−22	Cell adhesion molecules (CAMs)	12	6.65e−12
Lymphocyte activation	BP	22	2.61e−18	T cell receptor signaling pathway	10	2.38e−10
Leukocyte activation	BP	23	5.29e−18	Graft−versus−host disease	6	4.66e−08
Cell activation	BP	23	1.38e−16	Antigen processing and presentation	7	1.10e−07
T cell activation	BP	18	5.10e−16	Human immunodeficiency virus 1 infection	10	2.86e−07
Regulation of immune system process	BP	24	1.73e−15	Primary immunodeficiency	5	8.64e−07
Regulation of leukocyte activation	BP	16	2.04e−13	Hematopoietic cell lineage	6	5.27e−06
Adaptive immune response	BP	14	2.09e−13	Th1 and Th2 cell differentiation	6	9.45e−06
Positive regulation of immune system process	BP	19	2.47e−13	Human T−cell leukemia virus 1 infection	9	2.08e−05
Side of membrane	CC	20	3.30e−18	Th17 cell differentiation	6	2.26e−05
External side of plasma membrane	CC	16	6.50e−17	Viral myocarditis	5	2.95e−05
Cell surface	CC	19	4.95e−13	Chagas disease (American trypanosomiasis)	6	3.32e−05
Plasma membrane part	CC	29	6.90e−13	Autoimmune thyroid disease	4	3.51e−05
Plasma membrane	CC	35	3.83e−10	Allograft rejection	4	3.51e−05
Cell periphery	CC	35	8.41e−10	Cytokine−cytokine receptor interaction	7	5.53e−05
Membrane part	CC	37	6.76e−08	Type I diabetes mellitus	4	9.71e−05
Membrane	CC	45	1.03e−07	Human cytomegalovirus infection	7	3.32e−04
Immunological synapse	CC	5	1.39e−07	Chemokine signaling pathway	6	4.63e−04
T cell receptor complex	CC	4	2.73e−07	Measles	5	6.12e−04
Antigen binding	MF	6	5.62e−09	Epstein-Barr virus infection	6	1.16e−03
T cell receptor binding	MF	4	9.99e−08	Leukocyte transendothelial migration	4	3.10e−03
TAP binding	MF	3	3.09e−06	Human papillomavirus infection	7	4.05e−03
Beta-2-microglobulin binding	MF	3	4.63e−06	Herpes simplex infection	5	4.16e−03
MHC class I protein complex binding	MF	2	1.49e−05	Fc epsilon RI signaling pathway	3	6.22e−03
Receptor activity	MF	12	2.70e−05	Regulation of actin cytoskeleton	5	8.66e−03
Molecular transducer activity	MF	12	2.70e−05	Rheumatoid arthritis	3	9.47e−03
Peptide antigen binding	MF	3	3.03e−05	Cellular senescence	4	1.78e−02
Protein dimerization activity	MF	14	3.52e−05	NF-kappa B signaling pathway	3	1.97e−02
Cytokine receptor activity	MF	4	8.56e−05	Fc gamma R-mediated phagocytosis	3	1.97e−02

Structures were counted and labelled as cells based on user defined cut off values for cell size and circularity. Finally, the average number of cells per 512 × 512 frame is estimated. Macro available through: https://github.com/S-B-lab/confocal_image_quantifier.

2.17. Statistical analysis

Mean with 95% confidence interval or median with 25th–and 75th percentile range was presented when appropriate. *P*-values or false discovery rates < 0.05 were considered significant. Assumption of normality of data was evaluated using Shapiro Wilk's test. Assumption of homogeneity of variances between groups was evaluated using Fligner-Killeen's test. Interaction between dependent and independent continuous variables for categorical groups were investigated using a mixed ANOVA followed by one-way ANOVA of significant main effects followed by Tukey's post hoc test. When assumptions for ANOVA were not fulfilled, a Kruskal-Wallis H test with pair-wise Mann-Whitney *U* tests with Holm-Bonferroni correction was implemented. Independent two-group comparisons were conducted using Student's *t*-test or a Mann-Whitney U test depending on fulfillment of assumptions. Correlation between two continuous variables displaying a monotonic but not linear relationship was analyzed using Spearman's rank-order and Kendall's rank correlation. Sensitivity of key measures was evaluated using the ordinary bootstrap approach. Statistical analysis and plotting was done in R (version 3.3.2) mainly using packages 'data.table' and 'ggplot2'.

3. Results

3.1. Syngeneic, in contrast to allogeneic, MSCs suppress genes related to immune system response, pro-inflammation and microglia

We conducted global transcriptional analysis of injured spinal cords 20 days following treatment with allogeneic mesenchymal stem cells (SCI + aMSC) or syngeneic MSCs (SCI + sMSC) (Fig. 1A). SCI + sMSC and SCI + aMSC had different gene expression profiles, in relation to each other and to control (Fig. 1B, Suppl. Fig. 4A-B). SCI + sMSC was more similar to uninjured spinal cord while SCI + aMSC was more similar to SCI (Fig. 1C). Sixty-two genes were significantly differentially expressed between SCI + sMSC and SCI + aMSC (Fig. 1D). A majority of these genes were down-regulated in SCI + sMSC as compared to SCI + aMSC (Fig. 1E). Heat map representation confirmed the similarity between SCI + sMSC and uninjured spinal cords and the similarity between SCI + aMSC and SCI (Fig. 1F). Ten genes (APOBEC3, EPSTI1, AKNA, ITGAL, RAC2, H2-Q7, SASH3, PSMB8, IRF1, PIK3CD) explained most of the separation between SCI + sMSC and SCI + aMSC in the principal component analysis. Genes regulating pro-inflammatory cytokines/chemokines (CCL2–5, CXCL1, IL1β, TNFα) were down-regulated, as a group, in SCI + sMSC as compared to SCI + aMSC ($p < .001$) (Fig. 2A, C). This was also true for genes regulating microglia (FCRLS, HEXB, OLFML3, P2RY12, SALL1, TGFBR1, TMEM119) ($p < .001$) (Fig. 2B, D). Gene ontology terms related to immune system (e.g. immune system process, immune response, positive regulation of immune system process, leukocyte activation, regulation of leukocyte activation, lymphocyte activation, adaptive immune response, T cell activation) were down-regulated in SCI + sMSC as compared to SCI + aMSC (Fig. 2E, Table 3). This was also true for KEGG terms related to immune system (e.g. graft-versus-host disease, natural killer cell mediated cytotoxicity, allograft rejection, T cell receptor signaling pathway and cytokine-cytokine receptor interaction). Taken together, syngeneic MSCs, as compared to allogeneic MSCs, transplanted into injured spinal cord caused down-regulation of genes related to immune system response, pro-inflammation and microglia.

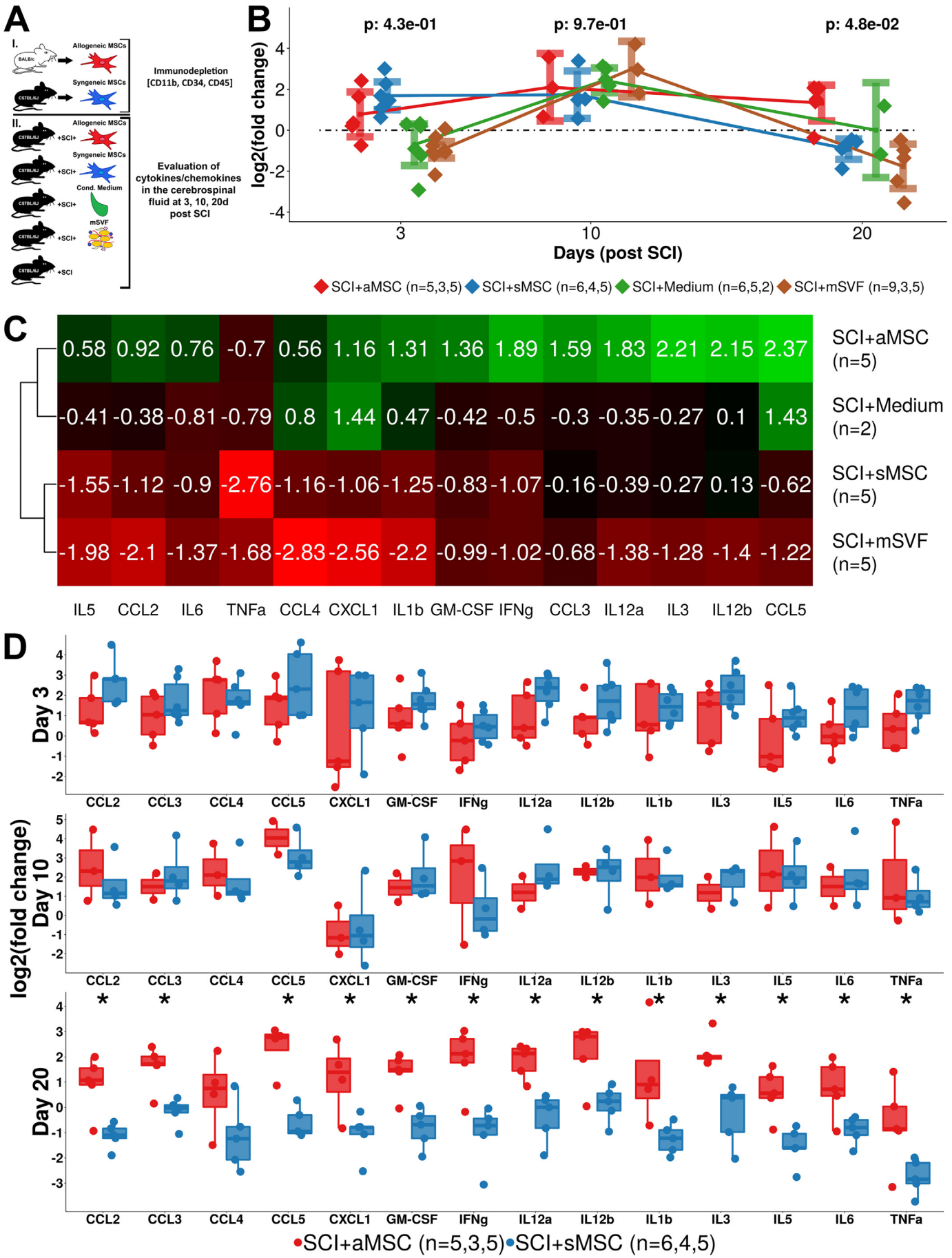

(caption on next page)

Fig 3. Expression of cytokines/chemokines in the cerebrospinal fluid following spinal cord injury.
Fig. 3A experimental design. I) Establishment of allogeneic mesenchymal stem cells (aMSC) and syngeneic MSCs (sMSC), II) experimental groups. Fig. 3B expression of pro-inflammatory cytokines/chemokines (TNFα, IL1β, IL6, CCL2, CCL3, CCL4, CCL5, IFNγ, CXCL1, IL12b, IL12a, IL3, IL5, GM-CSF) in the cerebrospinal fluid. Expression is reported as log2 of the fold change of expression in an experimental group in relation to the mean expression in animals with spinal cord injury (SCI) without treatment. Each dot represent one biological replicate. Mean values surrounded by 95% confidence intervals are reported. Numeric values are p-values for a post-hoc test between SCI + aMSC and SCI + sMSC following a multiple group comparison test between all experimental groups within each day. Fig. 3C agglomerative hierarchical clustering with heat map representation of the mean log2(fold change) for each experimental group and cytokine/chemokine at 20 days post SCI. Fig. 3D log2(fold change) for each cytokine/chemokine. Each dot represent one biological replicate. Significant differences following independent two-group comparisons are indicated (* = $p < .05$).

3.2. Syngeneic, in contrast to allogeneic, MSCs suppress expression of pro-inflammatory cytokines/chemokines

The inflammatory response following SCI is most often severe. Therefore, we investigated the impact of MSC transplantation on the expression of pro-inflammatory cytokines/chemokines in the cerebrospinal fluid (CSF) at 3, 10 and 20 days post SCI (Fig. 3A). At 3 days SCI + aMSC (0.77, CI: –0.32 – 1.86) and SCI + sMSC (1.68, CI: 1.00–2.36) had higher expression of pro-inflammatory cytokines/chemokines as compared to SCI, SCI + Medium and SCI + mSVF. However no difference between SCI + aMSC and SCI + sMSC could be detected ($p = .43$) (Fig. 3B). At 10 days SCI + aMSC and SCI + sMSC remained at a higher expression level of cytokine/chemokines as compared to SCI, and no difference between the groups could be detected ($p = .97$). At 20 days SCI + sMSC (-0.93, CI: –0.43 – -1.43) had a significantly lower expression of pro-inflammatory cytokines/chemokines as compared to SCI + aMSC (1.33, CI: 0.46–3.20) ($p < .05$) and to SCI ($p < .05$). At this time point SCI + mSVF had an expression profile lower than the SCI but similar to SCI + sMSC. At 20 days post SCI CCL2/3/5, GM-CSF, IFNγ, IL2a/b, IL1β/3/5/6, CXCL1 and TNFα were significantly down-regulated in SCI + sMSC as compared to SCI + aMSC (Fig. 3C, D). The difference in cytokine/chemokine expression at 20 days was robust in bootstrap sensitivity analysis in which SCI + aMSC (1.29, range: 1.18–1.40) had a significantly higher median expression as compared to SCI + sMSC (-0.92, range: -1.00 – -0.86) ($p < .05$) (Suppl. Fig. 4C-D). Analysis of gene expression of pro-inflammatory cytokines/chemokines in the spinal cord (Fig. 4A) at 3 and 10 days post SCI confirmed that no difference in mean expression was present between SCI + aMSCs and SCI + sMSCs ($p = .99$) (Fig. 4B). However, at 20 days SCI + sMSCs had a significantly lower expression of pro-inflammatory cytokines/chemokines as compared to SCI + aMSCs ($p = .05$). This difference was mainly explained CCL2, IL6 and IFNγ (Fig. 4C, D). This difference was robust in bootstrap sensitivity analysis in which SCI + aMSC (0.13, range: 0.02–0.25) had a higher mean expression as compared to SCI + sMSC (-1.15, range: -1.23 – -1.08) (Suppl. Fig. 4E-F). Taken together, syngeneic but not allogeneic MSCs suppressed expression of pro-inflammatory cytokines/chemokines in the CSF and in the spinal cord at 20 days post SCI.

3.3. Allogeneic MSCs activate microglia/macrophages classically while syngeneic MSCs activate microglia/macrophages alternatively

Polarization and activation of microglia-like macrophages and monocyte populations was investigated (Fig. 5A) in order to seek an explanation for the differences in inflammatory profile detected at 20 days post SCI (Fig. 3, Fig. 4). SCI + aMSC had a higher M1/M2 ratio (5.74) as compared to SCI + sMSC (4.85) 20 days post SCI (Fig. 5B). Resampling analysis confirmed a shift in median M1/M2 ratio between SCI + aMSC (5.74, range: 5.47–5.98) and SCI + sMSC (4.83, range: 4.53–5.12) (Suppl. Fig. 4G). Furthermore, the M1/M2 ratio was positively (ρ: 0.57; τ: 0.41) and significantly ($p < .001$) correlated with the expression of pro-inflammatory cytokines/chemokines in the spinal cord (Fig. 5C, Suppl. Fig. 4H). The M1/M2 ratio was also assessed in isolated microglia/macrophage ($CD11b^+CD45^{Low}Ly6G^-CD64^+$) and monocyte populations ($CD11b^+CD45^{High}Ly6G^-CD64^-$) (Fig. 5D). No difference in the number of microglia/macrophages or monocytes could be detected between SCI + aMSC and SCI + sMSC (Fig. 5E). However, the M1/M2 ratio was lower in microglia/macrophages populations isolated from SCI + sMSC (0.17, CI: –0.11 – 0.44) as compared to SCI + aMSC (1.01, CI: 0.41–1.62) ($p = .077$). Additionally SCI + sMSC had a lower M1/M2 ratio in isolated macrophages/microglia as compared to uninjured spinal cords ($p < .05$). No difference in M1/M2 ratio between monocyte-like populations could be detected (Fig. 5E). In order to investigate the activation of microglia/macrophages in more detail a histological examination of Iba1 + cells was conducted at 3, 10 and 20 days post SCI (Fig. 5F). At 3 days SCI + sMSC and SCI + aMSC suppressed activation of Iba1 + cells as compared to SCI ($p < .001$). However, no difference could be detected between the two experimental groups. At 10 days the activation of Iba1 + cells was lower in SCI + sMSC (22.26, CI: 16.03–28.49) as compared to SCI + aMSC (47.67, CI: 41.01–54.34) ($p = .055$). SCI + aMSC even had a higher activation as compared to SCI (24.55, CI: 19.59–29.51) ($p = .076$). Taken together, syngeneic as compared to allogeneic MSCs activate microglia-like macrophages alternatively and suppress macrophage activation both which correlates with lower expression levels of pro-inflammatory cytokines/chemokines post SCI.

3.4. Syngeneic, in contrast to allogeneic, MSCs enhance recovery of hind limb function

Recovery in hind limb function was estimated during the first 10 week post SCI using the iliac crest height index (ICHI) (Fig. 6A). SCI + sMSC and SCI + aMSC recovered significantly over time ($p < .001$) (Fig. 6B). SCI + Medium, SCI + mSVF and SCI did not recover significantly over time. SCI + sMSC had a higher rate of change in ICHI from day 3 to 35, as compared to SCI + aMSC. At steady state (42, 49, 70d post SCI) SCI + sMSC (1.41, CI: 1.37–1.46) had a significantly higher ICHI as compared to SCI + aMSC (1.24, CI: 1.19–1.29) ($p < .05$) (Fig. 6C). Resampling confirmed significantly higher ICHI at steady state for SCI + sMSC (1.41, range: 1.39–1.43) as compared to SCI + aMSCs (1.24, range: 1.22–1.26) (Suppl. Fig. 4I). At 70 days SCI + sMSC had significantly higher ICHI as compared to SCI + aMSC ($p = .075$), SCI + Medium ($p < .01$), SCI + mSVF ($p < .05$) and SCI ($p < .05$). Overall the trochanter major height index recovered to a higher extent in comparison to the ICHI (Fig. 6D). However, at steady state, no significant difference in trochanter major height index could be detected between SCI + sMSC (1.59, CI: 1.38–1.81) and SCI + aMSC (1.39, CI: 1.26–1.52). However, SCI + sMSC improved significantly in trochanter major height index in comparison to SCI + mSVF (1.14, CI: 1.03–1.25) and SCI + Medium (1.18, CI: 0.98–1.39). At sacrifice (70d post SCI) the neuronal survival was estimated in spinal cord sections in order to investigate the neuroprotective effect of MSCs. SCI + sMSC had a higher density of NeuN + cells (23.27, range: 17.00–29.53), as compared to SCI + aMSC (8.78, range: 8.60–8.95) and SCI (3.81, range: 1.34–6.28) (Fig. 6E). Taken together, syngeneic but not allogeneic MSCs enhance recovery in ICHI and contribute to neuronal survival.

3.5. Survival of syngeneic MSCs is superior to survival of allogeneic MSCs

In order to better understand the function of MSCs following transplantation the graft survival was investigated. Three days post SCI both allogeneic MSCs and syngeneic MSCs could be detected, and to the

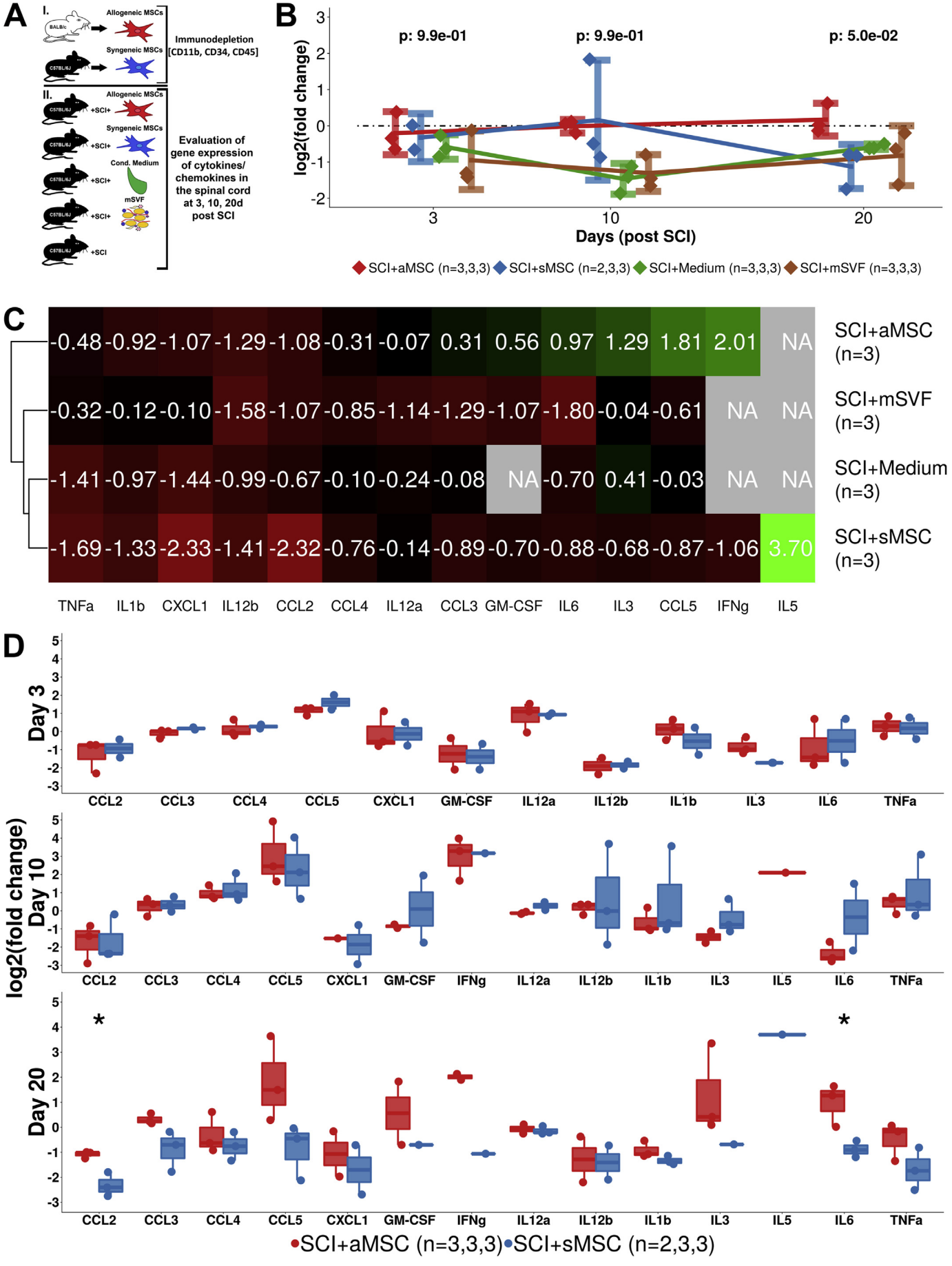

(caption on next page)

Fig 4. Expression of cytokines/chemokines in the spinal cord following spinal cord injury.
Fig. 4A experimental design. I) Establishment of allogeneic mesenchymal stem cells (aMSC) and syngeneic MSCs (sMSC), II) experimental groups. Fig. 4B expression of pro-inflammatory cytokines/chemokines (TNFα, IL1β, IL6, CCL2, CCL3, CCL4, CCL5, IFNγ, CXCL1, IL12b, IL12a, IL3, IL5, GM-CSF) in the spinal cord. Expression is reported as log2 of the fold change of expression in an experimental group in relation to the mean expression in animals with spinal cord injury (SCI) without treatment. Each dot represent one biological replicate. Mean values surrounded by 95% confidence intervals are reported. Numeric values are p-values for a post-hoc test between SCI + aMSC and SCI + sMSC experimental groups following a multiple group comparison test between all experimental groups within each day. Fig. 4C agglomerative hierarchical clustering with heat map representation of the mean log2(fold change) for each experimental group and cytokine/chemokine at 20 days post SCI. Fig. 4D log2(fold change) for each cytokine/chemokine. Each dot represent one biological replicate. Significant differences following independent two-group comparisons are indicated (* = $p < .05$).

same extent (Fig. 6F). Ten days post SCI the syngeneic MSCs were detected to a significantly higher extent (8.07, CI: 7.03–9.10) as compared to allogeneic MSCs (1.60, CI: 0.46–2.74) ($p < .05$). The survival of syngeneic MSCs at 10 days was similar to their survival at 3 days post SCI. Allogeneic MSCs had a significantly lower survival at 10 days as compared to their survival at 3 days post SCI ($p < .05$). No MSCs could be detected at 20 days post SCI in any of the two experimental groups. Taken together, syngeneic MSCs have superior survival as compared to allogenic MSCs at 10 days post SCI but no MSCs could be detected at 20 days post SCI in any of the experimental groups.

4. Discussion

This study aimed at assessing the importance of histocompatibility of transplanted mesenchymal stem cells (MSCs) for their therapeutic potential following SCI. We hypothesized that the therapeutic potential of syngeneic MSCs is superior to that of allogeneic MSCs. We found that syngeneic MSCs activated macrophages alternatively while allogeneic MSCs activated macrophages classically. This finding correlated with lower levels of pro-inflammatory cytokines/chemokines in animals treated with syngeneic MSCs as compared to animals treated with allogeneic MSCs. Additionally, syngeneic but not allogeneic MSCs down-regulated genes and pathways regulating the general immune response. Furthermore, syngeneic but not allogeneic, MSCs enhanced recovery of hind limb motor function, possibly by enhanced neuronal survival. Syngeneic MSCs also had a superior survival as compared to allogeneic MSCs. Thus, the results presented in this study suggest that the histocompatibility is of importance for the therapeutic potential of MSCs and these results therefore contradict the general assumption that MSCs are immune-privileged.

Syngeneic MSCs as compared to allogeneic MSCs down-regulated genes, gene sets and pathways related to the general immune response. A specific subset of genes (APOBEC3, EPSTI1, AKNA, ITGAL, RAC2, H2-Q7, SASH3, PSMB8, IRF1, PIK3CD) explaining the majority of the separation in the principal component analysis was identified. APOBEC3 has anti-viral activity, while AKNA can activate lymphocytes to undergo antigen-dependent-B-cell development. ITGAL can mediate cytotoxic T-cell mediated killing, and antibody dependent killing by granulocytes and monocytes but also contribute to natural killer cell cytotoxicity. H2-Q7 is involved in antigen presentation to the immune system, while IRF1 directly affects NK-cell maturation, IL12 expression from macrophages, maturation of CD8+ T-cells, suppress development of regulatory T-cells, differentiation and maturation of dendritic cells. Genes such as IL7, COX2, MHC-I and IL12a&b are targets for IRF1s transcriptional activity. PIK3CD expression contributes to T-cell development, expansion and differentiation of T-helper cells, aids the migration of NK-cells to the site of inflammation, activates NK cell receptors and contributes to the maturation of NK cells [ref: UniProt]. Taken together the syngeneic MSCs in comparison to allogeneic MSCs seem to suppress the function and activity of T –and NK cells which results in the syngeneic MSCs being able to suppress the immune response in general, following spinal cord injury.

It has consistently been reported that transplanted MSCs can down-regulate expression of pro-inflammatory cytokines/chemokines (Canton et al., 2013; Chen et al., 2015; Cízková et al., 2006; Friedenstein et al., 1974) and up-regulate expression of anti-inflammatory cytokines/chemokines (Shin et al., 2012). Most authors have documented a MSC-induced suppression of pro-inflammatory cytokines/chemokines occurs already at 7 days post SCI (Chen et al., 2015; Cízková et al., 2006). In our study, however, neither allogeneic MSCs nor syngeneic MSCs managed to suppress expression of pro-inflammatory cytokines/chemokines at 10 days post SCI. At 20 days post SCI however, syngeneic MSCs suppressed while allogeneic MSCs enhanced expression of pro-inflammatory cytokines/chemokines. This modulation of cytokine/chemokine expression was also described by Urdzíková et al. 2014 (Canton et al., 2013). Taken together, syngeneic MSCs modulate the inflammatory response favorably in comparison to allogeneic MSCs, but this effect does not become apparent until 20 days post SCI.

Expression of pro-inflammatory cytokine/chemokines is thought to be mediated by classically activated macrophages (M1: CD16+/32+) (Torres-Espín et al., 2015; Tse et al., 2003). Nakajima et al. 2012 reported that MSCs transplanted into SCI could not only reduce the number of classically activated macrophages but also enhance the number of alternatively activated macrophages (M2: Arg1+/CD206+). The authors found a positive correlation between the polarization and the expression of pro (IL6, TNFα) –and anti (IL4, IL13)-inflammatory cytokines/chemokines (Chan et al., 2008). These findings were confirmed by Urdzíková et al. in 2014 among others (Canton et al., 2013; Uccelli et al., 2008).

We documented that syngeneic MSCs lowered the M1/M2 ratio while allogeneic MSCs elevated the M1/M2 ratio in the spinal cord in general but also in microglia-like macrophages. A positive correlation between the M1/M2 ratio and the level of pro-inflammatory cytokines/chemokines was also detected. Taken together, syngeneic MSCs in comparison to allogeneic MSCs can alternatively activate microglia-like macrophages which results in the syngeneic MSCs being able to suppress the expression of pro-inflammatory cytokines/chemokines during the early chronic phase of SCI.

MSCs have a solid reputation for being able to contribute significantly to improvement of the hind limb function (Chen et al., 2015; Gu et al., 2010; Han et al., 2015; Himes et al., 2006; Isakova et al., 2014; Iwamoto et al., 1994; Jung et al., 2009; Kim et al., 2015; Klyushnenkova et al., 2005; Le Blanc et al., 2003; Liu et al., 2012; Martini et al., 2010; Melief et al., 2013). In this study, the hind limb function was measured by the iliac crest height index (ICHI). Grafting of syngeneic MSCs significantly enhanced the recovery in ICHI in comparison to a more modest recovery following transplantation of allogeneic MSCs. We also documented a significantly higher neuronal survival (NeuN+ cells) at 70 days post SCI in animals treated with syngeneic MSCs in comparison to animals treated with allogeneic MSCs. The superior recovery in hind limb function was negatively correlated with the level of M1/M2 ratio and level of pro-inflammation but positively correlated with neuronal survival. Hence the transplanted syngeneic MSCs might contribute to functional recovery through neuroprotection which in turn might result from a more beneficial immune system response. In this study we used an objective rather than a subjective functional outcome measure (e.g. basso mouse scale, BMS). The simple reason is that a subjective measure is heavily dependent on the scorers experience and knowledge, is resource intensive (requires independent blinded scorers) and requires the same amount of documentation/recordings as an objective evaluation. Evaluation in a

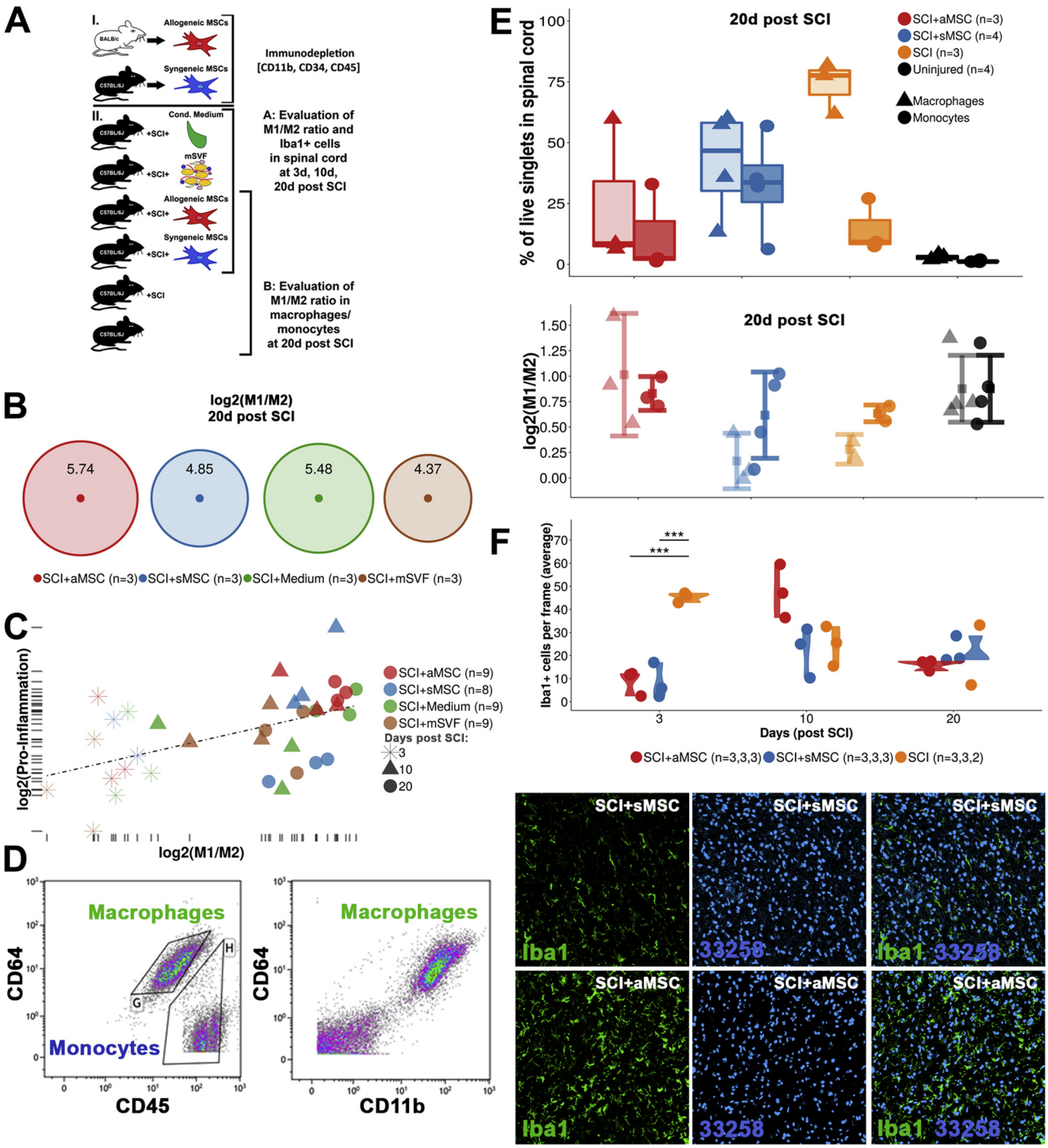

Fig. 5. Activation and polarization of microglia/macrophages and monocyte populations in the spinal cord following spinal cord injury.
Fig. 5A experimental design. I) Establishment of allogeneic mesenchymal stem cells (aMSC) and syngeneic MSCs (sMSC), II) experimental groups. Fig. 5B log2(M1/M2) at 20 days post spinal cord injury (SCI) (M1: CD16+ AND CD32+, M2: CD206+ AND Arg1+). Fig. 5C linear relation between mean log2(M1/M2) and mean level of log2(pro-inflammation) for each biological replicate. Fig. 5D gate used for isolation of microglia-like macrophages ($CD11b^{+}CD45^{Low}Ly6G^{-}CD64^{+}$) and monocyte-like cells ($CD11b^{+}CD45^{High}Ly6G^{-}CD64^{-}$) using fluorescence activated cell sorting. Fig. 5E percentage of microglia-like macrophages and monocyte-like cells in spinal cord (% of live singlets) at 20 days post SCI. Log2(M1/M2) in isolated microglia-like macrophages and monocyte-like cells at 20 days post SCI. Each dot represents one biological replicate. Fig. 5F average number of Iba1+ cells per confocal image (20×) (*** = $p < .001$). Each dot represents one biological replicate. Representative images of Iba1+ cells in spinal cord sections for SCI + sMSC and SCI + aMSC experimental groups at 10 days post SCI.

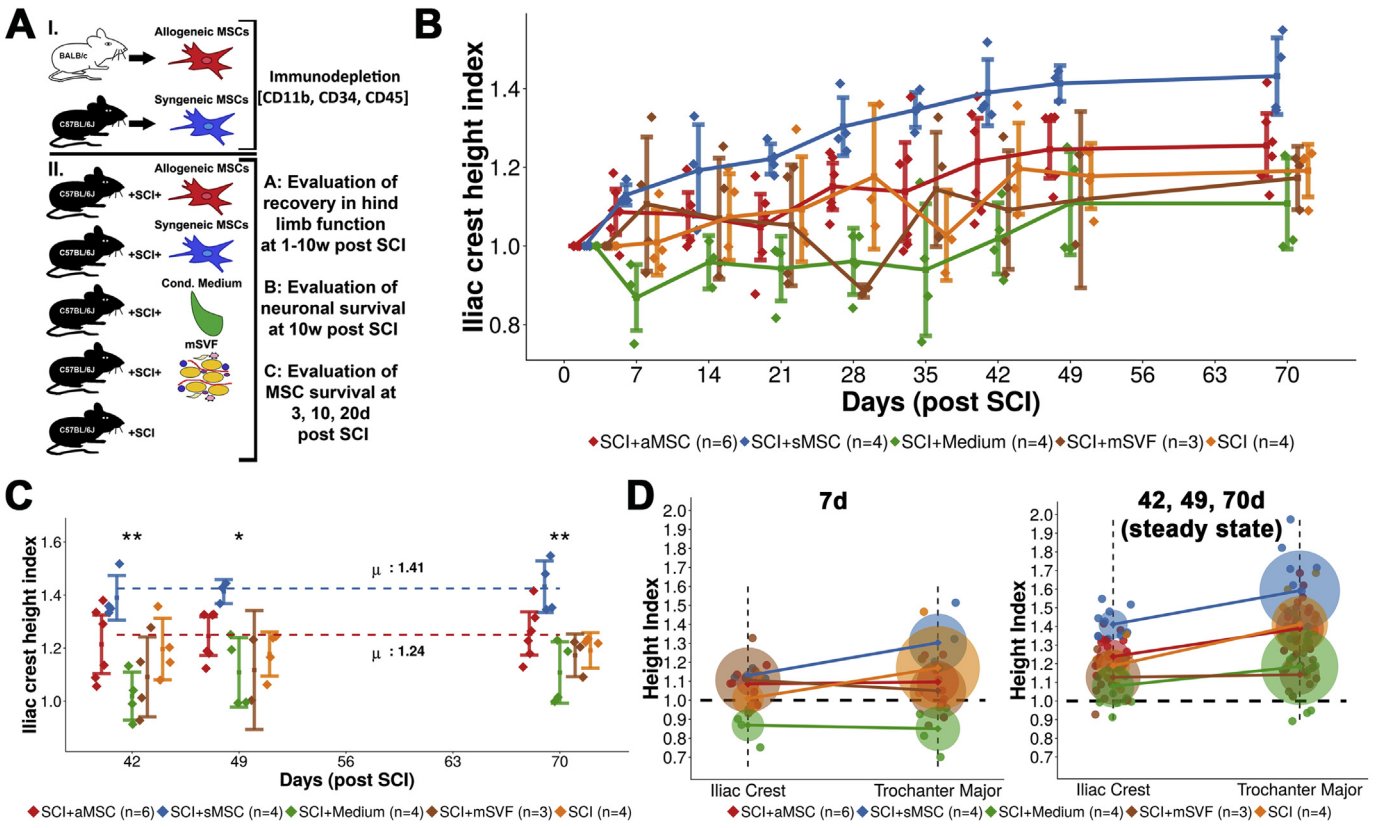

(caption on next page)

Fig. 6. Hind limb function following spinal cord injury.
Fig. 6A experimental design. I) Establishment of allogeneic mesenchymal stem cells (aMSC) and syngeneic MSCs (sMSC), II) experimental groups. Fig. 6B iliac crest height index (ICHI). ICHI defined as the ratio between the iliac crest height at time points > 3 days divided by the mean iliac crest height at 3 days post spinal cord injury (SCI), calculated for each biological replicate separately. Mean surrounded by a 95% confidence interval. Fig. 6C ICHI at steady state. Horizontal line is the mean ICHI for SCI + sMSC and SCI + aMSC groups at all three time points taken together. Significance of multiple group comparison test between groups within days are reported (* = $p < .05$, ** = $p < .01$). Fig. 6D ICHI and the trochanter major height index. Circles represent 95% confidence intervals around the mean height index. Each dot represents a biological replicate. Lines connect the mean values between the two height indices. Fig. 6E mean number of NeuN+ cells per confocal frame in spinal cord sections. Each dot represents one biological replicate. Representative images of NeuN+ cells counterstained with Hoechest 33258 in spinal cord sections for SCI + sMSC and SCI + aMSC groups at 70 days post SCI. Fig. 6F mean number of mCherry+MSCs per confocal frame in spinal cord sections for SCI + sMSC and SCI + aMSC groups. Each dot represents one biological replicate. Significance of independent two-group comparison reported (* = $p < .05$). Representative images of mCherry+MSCs counterstained with Hoechest 33258 in spinal cord sections for SCI + sMSC and SCI + aMSC groups at 10 days post SCI.

walking tunnel with post-hoc evaluation of measurement such as distances/heights, angles and stepping pattern allows for evaluation of more parameters in comparison to a subjective measurement.

The reporting on the survival of grafted MSCs has been contradictory. While some authors have documented a significant survival (Urdzíková et al., 2014; Zangi et al., 2009; Zhou et al., 2016; Zörner et al., 2010), others have obtained opposite results (Kim et al., 2015; Shin et al., 2012). Jung et al. 2009 reported that although both syngeneic MSCs and allogeneic MSCs have been detected up to four weeks post SCI, the survival rate of syngeneic MSCs is superior to allogeneic MSCs (Urdzíková et al., 2014). Zangi et al. 2009 confirmed this finding. The authors reported that MSCs are not immune-privileged and are rejected under allogeneic settings which is followed by an immune memory (Prigozhina et al., 2008). Prigozhina et al. 2008 reported that while allogeneic MSCs were rejected regardless of origin, syngeneic MSCs were not (Prigozhina et al., 2008; Quertainmont et al., 2012). We documented similar survival between allogeneic MSCs and syngeneic MSCs in the acute phase of the SCI. However, during the subacute phase, syngeneic MSCs had superior survival. It is obvious that the cells need not to be present for a protracted period of time for the hind limb function to improve, as demonstrated in this study. We hypothesize that the beneficial modulations of the immune response mediated by the syngeneic MSCs observed in this study are sufficient for improving the functional recovery. It is widely accepted in the field that MSCs act through paracrine effects and most possibly through secretion of extracellular vesicles, by which they modify the surrounding tissue beneficially and that graft survival is not likely or necessary. Taken together, both allogeneic and syngeneic MSCs perish with time but allogeneic MSCs perish prior to syngeneic MSCs. The reason for the disappearance however, was not investigated but could be immune-system mediated rejection, lack of micro-environmental support or simply fading of the fluorescence.

Allogeneic MSC transplantation was only performed in one direction (MSC from BALB/c to C57BL/6 J mice). We cannot rule out the possibility that a reverse model in which MSCs from C57BL/6 J transplanted into BALB/c mice would yield different results than those presented. This is however unlikely considering that it is widely known in the field that MSCs from BALB/c have superior growth potential in culture conditions and the MSCs from BALB/c should in theory be superior to MSCs from C57BL/6 J, which they were not. Moreover, the MHC mismatch is the same regardless of transplantation direction. However, the results in this project are only valid for these two strains of mice and the implemented definition of allogeneic MSCs and their direction of transplantation.

Animal surgery, SCI induction, MSc transplantation and placement of markers during iliac crest and trochanter major height evaluation are procedures which are subject to potential experimenter bias. The variation in surgical technique, induction of SCI and cell transplantation was reduced by having one single individual performing all the experiments. This individuals has extensive experience of animal care, surgery and cell transplantation. Therefore, it is not likely that the individual significantly improved his skills over time thereby introducing a bias. Moreover, the SCI was induced using a commercially available standardized contusion apparatus (IH-0400) and all data related to each impact was saved. Additionally, the SCI was induced with the spinal column fixated and stabilized in a stereotaxic frame. This minimizes variations in injury severity in terms of tissue damage and impact on the corticospinal tract. Cell transplantation is perhaps the most difficult part and therefore probably the largest source of error. These were also performed by the same individual, who has great experience in transplanting various types of stem cells to spinal cord. The labelling of the anatomical land marks, which were used for iliac crest and trochanter major height measurements are in fact not necessary. These anatomical land marks can easily be recognized visually in the recordings of the animals, which are saved and stored. This implies that the placement of the markers cannot easily be biased by the person placing them.

We conclude that syngeneic MSCs, but not allogeneic MSCs, can suppress expression of pro-inflammatory cytokines/chemokines by alternatively activating macrophages and by down-regulating the immune response in general. Syngeneic MSCs but not allogeneic MSCs contribute to improvement in hind limb motor function and also have superior survival. Hence, the common assumption that MSCs regardless of origin and type are immune-privileged might have to be re-considered. Transplantation of allogeneic MSCs in the acute phase might have to be supplemented or combined with other treatments in order to counteract or reduce the potential negative impact detected in this study. One potential approach for solving this problem would be to understand and exploit the mechanism of action of MSCs in order to bypass the need for cell transplantation.

Supplementary data to this article can be found online at https://doi.org/10.1016/j.jneuroim.2018.11.005.

Funding

The Swedish Medical Research Council, The Swedish Society of Medicine, Karolinska Institutet, Swedish Brain Foundation, Stockholm City Council.

Declarations of interest

None.

References

Ahuja, C.S., Wilson, J.R., Nori, S., et al., 2017. Traumatic spinal cord injury. Nat Rev Dis Primers 3, 17018.
Araña, M., Mazo, M., Aranda, P., Pelacho, B., Prosper, F., 2013. Adipose tissue-derived mesenchymal stem cells: isolation, expansion, and characterization. Methods Mol. Biol. 1036, 47–61.
Aras, Y., Sabanci, P.A., Kabatas, S., et al., 2016. The effects of adipose tissue-derived mesenchymal stem cell transplantation during the acute and subacute phases following spinal cord injury. Turk Neurosurg 26, 127–139.
Berglund, A.K., Schnabel, L.V., 2017 Jul. Allogeneic major histocompatibility complex-mismatched equine bone marrow-derived mesenchymal stem cells are targeted for death by cytotoxic anti-major histocompatibility complex antibodies. Equine Vet. J. 49 (4), 539–544.
Cantinieaux, D., Quertainmont, R., Blacher, S., et al., 2013. Conditioned medium from bone marrow-derived mesenchymal stem cells improves recovery after spinal cord injury in rats: an original strategy to avoid cell transplantation. PLoS One 8, e69515.
Canton, J., Neculai, D., Grinstein, S., 2013. Scavenger receptors in homeostasis and immunity. Nat Rev Immunol 13, 621–634.
Chan, W.K., Lau, A.S., Li, J.C., Law, H.K., Lau, Y.L., Chan, G.C., 2008. MHC expression

kinetics and immunogenicity of mesenchymal stromal cells after short-term IFN-gamma challenge. Exp. Hematol. 36, 1545–1555.
Chen, Y.B., Jia, Q.Z., Li, D.J., et al., 2015. Spinal cord injury in rats treated using bone marrow mesenchymal stem-cell transplantation. Int. J. Clin. Exp. Med. 8, 9348–9354.
Cízková, D., Rosocha, J., Vanický, I., Jergová, S., Cízek, M., 2006. Transplants of human mesenchymal stem cells improve functional recovery after spinal cord injury in the rat. Cell. Mol. Neurobiol. 26, 1167–1180.
Friedenstein, A.J., Chailakhyan, R.K., Latsinik, N.V., Panasyuk, A.F., Keiliss-Borok, I.V., 1974. Stromal cells responsible for transferring the microenvironment of the hemopoietic tissues. Cloning in vitro and retransplantation in vivo. Transplantation 17, 331–340.
Gu, W., Zhang, F., Xue, Q., Ma, Z., Lu, P., Yu, B., 2010. Transplantation of bone marrow mesenchymal stem cells reduces lesion volume and induces axonal regrowth of injured spinal cord. Neuropathology 30, 205–217.
Han, D., Wu, C., Xiong, Q., Zhou, L., Tian, Y., 2015. Anti-inflammatory mechanism of bone marrow mesenchymal stem cell transplantation in rat model of spinal cord injury. Cell Biochem. Biophys. 71, 1341–1347.
Himes, B.T., Neuhuber, B., Coleman, C., et al., 2006. Recovery of function following grafting of human bone marrow-derived stromal cells into the injured spinal cord. Neurorehabil. Neural Repair 20, 278–296.
Isakova, I.A., Lanclos, C., Bruhn, J., et al., 2014. Allo-reactivity of mesenchymal stem cells in rhesus macaques is dose and haplotype dependent and limits durable cell engraftment in vivo. PLoS One 9, e87238.
Iwamoto, R., Higashiyama, S., Mitamura, T., Taniguchi, N., Klagsbrun, M., Mekada, E., 1994. Heparin-binding EGF-like growth factor, which acts as the diphtheria toxin receptor, forms a complex with membrane protein DRAP27/CD9, which up-regulates functional receptors and diphtheria toxin sensitivity. EMBO J. 13, 2322–2330.
Jung, D.I., Ha, J., Kang, B.T., et al., 2009. A comparison of autologous and allogenic bone marrow-derived mesenchymal stem cell transplantation in canine spinal cord injury. J. Neurol. Sci. 285, 67–77.
Kim, Y., Jo, S.H., Kim, W.H., Kweon, O.K., 2015. Antioxidant and anti-inflammatory effects of intravenously injected adipose derived mesenchymal stem cells in dogs with acute spinal cord injury. Stem Cell Res Ther 6, 229.
Klyushnenkova, E., Mosca, J.D., Zernetkina, V., et al., 2005. T cell responses to allogeneic human mesenchymal stem cells: immunogenicity, tolerance, and suppression. J. Biomed. Sci. 12, 47–57.
Le Blanc, K., Tammik, C., Rosendahl, K., Zetterberg, E., Ringdén, O., 2003. HLA expression and immunologic properties of differentiated and undifferentiated mesenchymal stem cells. Exp. Hematol. 31, 890–896.
Liu, H., Lu, K., MacAry, P.A., et al., 2012. Soluble molecules are key in maintaining the immunomodulatory activity of murine mesenchymal stromal cells. J. Cell Sci. 125, 200–208.
Martini, M., Testi, M.G., Pasetto, M., et al., 2010. IFN-gamma-mediated upmodulation of MHC class I expression activates tumor-specific immune response in a mouse model of prostate cancer. Vaccine 28, 3548–3557.
Melief, S.M., Schrama, E., Brugman, M.H., et al., 2013. Multipotent stromal cells induce human regulatory T cells through a novel pathway involving skewing of monocytes toward anti-inflammatory macrophages. Stem Cells 31, 1980–1991.
Melo, F.R., Bressan, R.B., Forner, S., et al., 2017 Jul. Transplantation of human skin-derived mesenchymal stromal cells improves locomotor recovery after spinal cord injury in rats. Cell. Mol. Neurobiol. 37 (5), 941–947.
Menezes, K., Nascimento, M.A., Gonçalves, J.P., et al., 2014. Human mesenchymal cells from adipose tissue deposit laminin and promote regeneration of injured spinal cord in rats. PLoS One 9, e96020.
Morita, T., Sasaki, M., Kataoka-Sasaki, Y., et al., 2016. Intravenous infusion of mesenchymal stem cells promotes functional recovery in a model of chronic spinal cord injury. Neuroscience 335, 221–231.
Naglich, J.G., Metherall, J.E., Russell, D.W., Eidels, L., 1992. Expression cloning of a diphtheria toxin receptor: identity with a heparin-binding EGF-like growth factor precursor. Cell 69, 1051–1061.
Nakajima, H., Uchida, K., Guerrero, A.R., et al., 2012. Transplantation of mesenchymal stem cells promotes an alternative pathway of macrophage activation and functional recovery after spinal cord injury. J. Neurotrauma 29, 1614–1625.
Okuda, A., Horii-Hayashi, N., Sasagawa, T., et al., 2017. Bone marrow stromal cell sheets may promote axonal regeneration and functional recovery with suppression of glial scar formation after spinal cord transection injury in rats. J Neurosurg Spine 26, 388–395.
Osaka, M., Honmou, O., Murakami, T., et al., 2010. Intravenous administration of mesenchymal stem cells derived from bone marrow after contusive spinal cord injury improves functional outcome. Brain Res. 1343, 226–235.
Park, S.I., Lim, J.Y., Jeong, C.H., et al., 2012. Human umbilical cord blood-derived mesenchymal stem cell therapy promotes functional recovery of contused rat spinal cord through enhancement of endogenous cell proliferation and oligogenesis. J Biomed Biotechnol 2012, 362473.
Prigozhina, T.B., Khitrin, S., Elkin, G., Eizik, O., Morecki, S., Slavin, S., 2008. Mesenchymal stromal cells lose their immunosuppressive potential after allotransplantation. Exp. Hematol. 36, 1370–1376.
Quertainmont, R., Cantinieaux, D., Botman, O., Sid, S., Schoenen, J., Franzen, R., 2012. Mesenchymal stem cell graft improves recovery after spinal cord injury in adult rats through neurotrophic and pro-angiogenic actions. PLoS One 7, e39500.
Ritfeld, G.J., Nandoe Tewarie, R.D., Vajn, K., et al., 2012. Bone marrow stromal cell-mediated tissue sparing enhances functional repair after spinal cord contusion in adult rats. Cell Transplant. 21, 1561–1575.
Ryu, H.H., Kang, B.J., Park, S.S., et al., 2012. Comparison of mesenchymal stem cells derived from fat, bone marrow, Wharton's jelly, and umbilical cord blood for treating spinal cord injuries in dogs. J. Vet. Med. Sci. 74, 1617–1630.
Schnabel, L.V., Pezzanite, L.M., Antczak, D.F., Felippe, M.J., Fortier, L.A., 2014. Equine bone marrow-derived mesenchymal stromal cells are heterogeneous in MHC class II expression and capable of inciting an immune response in vitro. Stem Cell Res Ther 5, 13.
Schu, S., Nosov, M., O'Flynn, L., et al., 2012. Immunogenicity of allogeneic mesenchymal stem cells. J. Cell. Mol. Med. 16, 2094–2103.
Shin, T., Ahn, M., Matsumoto, Y., 2012. Mechanism of experimental autoimmune encephalomyelitis in Lewis rats: recent insights from macrophages. Anat Cell Biol 45, 141–148.
Torres-Espín, A., Redondo-Castro, E., Hernandez, J., Navarro, X., 2015. Immunosuppression of allogenic mesenchymal stem cells transplantation after spinal cord injury improves graft survival and beneficial outcomes. J. Neurotrauma 32, 367–380.
Tse, W.T., Pendleton, J.D., Beyer, W.M., Egalka, M.C., Guinan, E.C., 2003. Suppression of allogeneic T-cell proliferation by human marrow stromal cells: implications in transplantation. Transplantation 75, 389–397.
Uccelli, A., Moretta, L., Pistoia, V., 2008. Mesenchymal stem cells in health and disease. Nat Rev Immunol 8, 726–736.
Urdzíková, L.M., Růžička, J., Labagnara, M., et al., 2014. Human mesenchymal stem cells modulate inflammatory cytokines after spinal cord injury in rat. Int. J. Mol. Sci. 15, 11275–11293.
Zangi, L., Margalit, R., Reich-Zeliger, S., et al., 2009. Direct imaging of immune rejection and memory induction by allogeneic mesenchymal stromal cells. Stem Cells 27, 2865–2874.
Zhou, H.L., Zhang, X.J., Zhang, M.Y., Yan, Z.J., Xu, Z.M., Xu, R.X., 2016. Transplantation of human amniotic mesenchymal stem cells promotes functional recovery in a rat model of traumatic spinal cord injury. Neurochem. Res. 41, 2708–2718.
Zörner, B., Filli, L., Starkey, M.L., et al., 2010. Profiling locomotor recovery: comprehensive quantification of impairments after CNS damage in rodents. Nat. Methods 7, 701–708.